Newborns and preterm infants at term equivalent age: A semi-quantitative assessment of cerebral maturity

Marie P. Pittet[a,b,*,#], Lana Vasung[a,c,#], Petra S. Huppi[a], Laura Merlini[d]

[a] Division of Development and Growth, Department of Child and Adolescent Medicine, Geneva University Hospitals, Geneva, Switzerland
[b] Division of Neurology, Department of Paediatrics, The Hospital for Sick Children, Toronto, ON, Canada
[c] Division of Newborn Medicine, Department of Paediatrics, Boston Children's Hospital, Harvard Medical School, Boston, MA, United States
[d] Paediatric Radiology Unit, Division of Radiology, Geneva University Hospitals, Geneva, Switzerland

ABSTRACT

Background and purpose: Currently available MRI scoring systems of cerebral maturation in term and preterm infant at term equivalent age do not include the changes of transient fetal compartments that persist to term age. We studied the visibility and the pattern of these structures in healthy term newborns compared to preterm infants at term equivalent age in order to investigate if they can be included in a new MRI score system. We hypothesized that transient fetal compartments are different in both groups, and that these differences can be characterized using the clinical T2-weighted MRIs.
Materials and methods: Using 3T MRI T2-weighted brain sequences of 21 full-term and 41 preterm infants (< 32 weeks), scanned at term equivalent age, 3 raters independently scored the maturation level of 3 transient fetal compartments: the periventricular crossroads, von Monakow segments of the white matter, and the subplate compartment. These 3 new items were included in a scoring system along with validated parameters of brain maturation (germinal matrix, bands of migration, subarachnoid space and quality of gyrification). A cumulative maturity score was calculated separately for both groups of newborns by adding together each item. More mature were the brain structures, higher was the cumulative maturity score.
Results: Cumulative maturity score distinguished full-term from preterm infants (mean score 41/60 ± 1.4 versus 37/60 ± 2.5 points, p < 0.001), with an increase of 0.5 points for each supplemental gestational week at birth (r = 0.5, 95% CI 0.5 – 0.85). While a majority of transient fetal compartments were less mature in preterm group at term equivalent age, von Monakow segments of the white matter and subplate compartment presented a more advanced maturational stage in the preterm group compared to the term group. No subject had all scored items in the most mature state. Except a slight intra-rater agreement for von Monakow segment II, inter- and intra-rater agreements were moderate to excellent indicating the potential of the developed scoring system in routine clinical practice.
Conclusion: Brain transient fetal structures can be assessed on regular T2-weighted MRI in newborns. Their appearance differs between term and preterm babies. However our results suggest a more complex situation, with both delayed and accelerated maturation pattern in preterm infants. It remains to be determined if these differences could be biomarkers of the future neurodevelopment of preterm infants.

1. Introduction

In the recent years MRI has become a major clinical tool for assessing the brain integrity during the neonatal period. In utero or early postnatal injury of the brain in development has been associated with the neurodevelopmental disabilities in the later life. In addition, even in the absence of visible brain lesions on MRI, a considerable number of preterm children (Schmidt et al., 2015) still exhibit neurodevelopmental disabilities. It has been suggested that the impaired or the abnormal brain maturation is a biological substrate of these disabilities

([Chau et al., 2013](); [Inder et al., 2003](); [Perlman, 2001]()).

In the previous years, numerous MRI parameters (e.g. spatio-temporal progression of myelination, degree of cortical folding, visibility of migrating cells, and quantitative assessment of germinal matrix remnants) ([Kidokoro et al., 2014](); [van der Knaap et al., 1996](); [Vossough et al., 2013](); [Woodward et al., 2006]()) were used in order to assess the level of cerebral maturity in preterm neonates (PN) at term equivalent age (TEA) ([Childs et al., 2001](); [Ferrie et al., 1999](); [George et al., 2015](); [Kidokoro et al., 2014](); [Nguyen The Tich et al., 2009](); [Ramenghi et al., 2011](); [Vossough et al., 2013](); [Walsh et al., 2014]()). However, the semiquantitative maturation scores derived from using these parameters do not take into account the existence or disappearance of transient fetal compartments, that are characteristic of normal human brain maturation. In particular, MRI characteristics of transient fetal compartments such as the subplate compartment and the intermediate zone were never assessed in PN at TEA.

During the early (23-29 gestational weeks (GW)) and the late preterm (29-34 GW) periods axonal pathways navigate through the transient fetal compartments ([Takahashi et al., 2012](); [Vasung et al., 2010](); [Vasung et al., 2017]()), periventricular crossroad areas ([Judas et al., 2005]()), and "wait" in the subplate compartment before they enter the cortical plate ([Ivica and Judas, 2007](); Kostovic and Judas, 2006). The transient subplate compartment is also a site of neuronal differentiation, synaptogenesis, axonal guidance which reaches its peak volume and thickness around 32 GW ([Vasung et al., 2016]()). The decline in the thickness of the subplate compartment, which occurs during the last few weeks of the pregnancy, coincides with the re-organisation of the fetal white matter (WM) into the von Monakow segments ([Ivica et al., 2014](); [Vasung et al., 2010](); [von Monakow, 1905]()). In addition, during this period the cortical convolutions (gyri and sulci) become more complex ([Chi et al., 1977](); [Dubois et al., 2008a](); [Dubois et al., 2008b]()). The intense developmental activity of the transient fetal compartments during the second half of gestation makes them vulnerable to endogenous and exogenous insults due to a premature birth (ischemia, inflammation, excitotoxicity). We hypothesized that imaging characteristics of these transient fetal compartments could be key-bio-markers of altered brain development in PN at TEA. The rationale driving our hypothesis lies on the match previously reported between the T2w MRI and structural, histological and immunocytochemical descriptions of the transient fetal compartments in the normal fetuses ([Ivica et al., 2014](); [Ivica and Judas, 2010](); [Judas et al., 2005](); [Vasung et al., 2016]()). To our knowledge, the MRI characteristics of the transient fetal compartments in the term newborns (TN) and the PN at TEA have not been described.

In this current study, we have retrospectively reviewed standard T2w MRI brain scans of TN and PN at TEA to specifically assess these transient structures. The first aim of our work was to explore if these transient fetal compartments are easily visible in newborns with a good intra- and inter-reader agreement by radiologists and paediatricians. Secondly, we investigated if there is a "normal" maturation pattern based on the aspect of these structures in TN. Thirdly, we examined if differences exist in the maturation level of transient fetal brain structures between healthy TN and PN at TEA. We thus elaborated a score of brain maturity that includes these transient fetal structures along with scoring parameters already established in the literature such as germinal matrix, bands of migrating glial cells, subarachnoid space and quality of gyrification.

2. Materials and methods

Institutional Review Board approved the study and informed consent was obtained from both parents. We retrospectively included 41 PN at TEA ($\geq$ 38 to $\leq$ 42 GW) and 21 healthy TN. Estimated gestational age was based on the first day of the mothers last menstrual period. Exclusion criteria included inadequate MR imaging data quality, chromosomal abnormalities, congenital infection, focal brain abnormalities on MRI and congenital heart defects. All subjects were born at the University Hospital of Geneva between 2007 and 2014.

2.1. Clinical data

All clinical data were retrospectively collected from infant electronic medical records.

2.2. MRI data acquisition

TN underwent MR-imaging during the first few days of life (range 1-5 days), PN at TEA, on a 3T Siemens TrioTim system (Siemens Medical Solutions, Erlangen, Germany) with a MR scan protocol adapted for the newborns ([Gui et al., 2012]()). MR images were acquired during the newborns' post-prandial sleep without the use of sedation. The infants were swaddled and placed in a vacuum pillow that was designed to keep the infant still. In order to reduce the noise exposure special mini-muffs were applied on their ears. A pulse oximeter was used to monitor the patient throughout the imaging procedure. Images that were used for neuro-radiological reading were high-resolution T2-weighted (T2w) MR images (TE = 2.91 ms, TR = 2500 ms, TI = 1100 ms, with the voxel resolution of $0.8 \times 0.8 \times 1.2$ mm^3).

2.3. Image analysis

Before the scoring, we selected T2w MR images that were free from motion artefacts. 3D T2w MR images were read using the OsiriX® software (Pixmeo, Geneva, Switzerland). Three readers with different medical backgrounds (L.V as MD with an expertise in developmental neuroanatomy and experience in neuroradiology, L.M as an experienced paediatric radiologist, and M.P. as child neurologist) read the MRI. The readers were blinded to the clinical data. After 4 months, in order to assess the intra-observer reliability, two readers (L.M, M.P) repeated the MRI readings in half of the subjects. The MRIs were blinded and the order of subjects was rearranged upon the second reading.

2.4. Development of the grading system for assessment of the brain maturity level

We used a standardized grading system that was developed for this study. A 2 or 3-point scale was used to assess the level of maturity. Higher number was attributed to the more mature structure. Some components (subarachnoid space, gyrification, bands of migration, germinal matrix) were inspired by previously published postnatal scoring system developed to assess the brain maturity in newborns ([Woodward et al., 2006]()) while others (crossroads, von Monakow segments, subplate compartment) were based on the histological and ex vivo MRI descriptions of transient fetal structures ([Judas et al., 2005](); Kostovic and Vasung, 2009; Krsnik et al., 2017; [Pogledic et al., 2014]()).

To respect the maturational asynchrony of the brain in development, the grading of the fetal structures was done in the different regions of the brain. Frontal, central, and parietal regions were evaluated using the coronal slices that were perpendicular to the anterior commissure-posterior commissure line (AC-PC line). Frontal regions were evaluated on the coronal slices passing through the most rostral tip of lateral ventricles. Central regions were evaluated on the coronal slices passing through the third ventricle and the cerebral aqueduct of Sylvius. Parietal regions, that are located above the antrum and occipital horns of lateral ventricle, were evaluated on the coronal slices passing through the calcarine fissure.

We have separately graded the level of maturity of the white matter, gray matter, and the subplate compartment:

- the grading of the WM maturity level was based on estimating the visibility of transient fetal structures: i) periventricular crossroads,
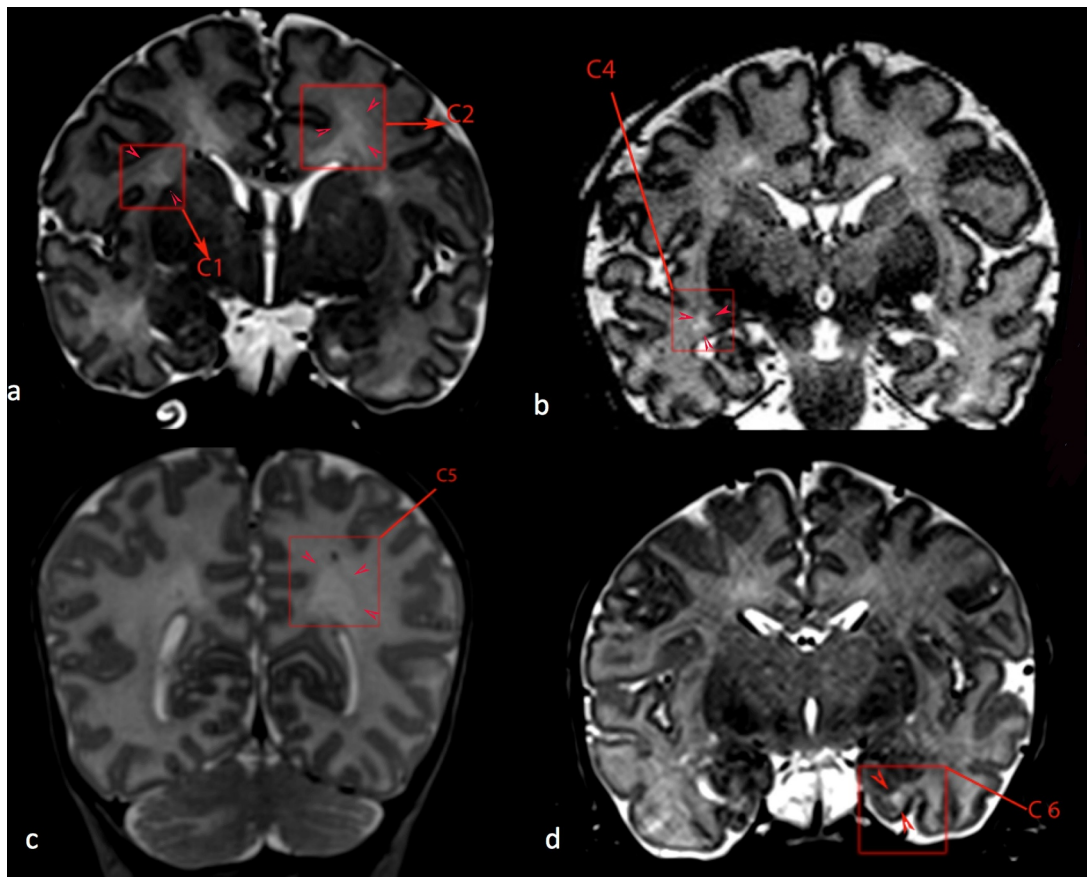
Fig. 1. Periventricular crossroad areas (red squares). T2w MRI coronal slices of central (**a, b, d**) and posterior (**c**) regions of the brain. Both C1 and C2 periventricular crossroad areas are located in the proximity of the anterior horn of the lateral ventricles. C1 crossroad is located lateral, while C2 is located above the anterior horn of lateral ventricles (**a**). C4 periventricular crossroad area has a triangular shape and is located at the exit of the retro-ventricular portion of the posterior limb of the internal capsule (**b**). C5 periventricular crossroad area is located dorsolateral to the posterior horn of the lateral ventricle, close to the parieto-occipital junction (**c**). C6 periventricular crossroad area is located anterolateral to the tip of the inferior horn of the lateral ventricle (**d**).(For interpretation of the references to colour in this figure legend, the reader is referred to the web version of this article.)

ii) von Monakow segments, and iii) periventricular band of the migrating cells.

- the level of maturity of the gray matter was based on visibility of the germinal matrix and the estimated level of gyrification.
- the maturity of the subplate compartment was assessed separately as this zone is crucial for the organization of the both white and gray matter.
- finally, we have also measured the thickness of CSF in the subarachnoid space.

Levels of maturity of the WM, gray matter, subplate compartment, and the width of subarachnoid space were added together in a final number, which, as we hypothesized, would reflect a global level of maturity of the newborn brain. The highest possible cumulative score was 60 and not expected to be reached before 6 months of age.

2.4.1. Grading the white matter level of maturity

2.4.1.1. Crossroad areas.
Based on the *ex vivo* MRI and histology, six periventricular crossroad areas (C1 to C6) have been described in the fetal and neonatal human brain. All of the crossroad areas are located along the lateral wall of the lateral ventricles (Fig. 1). The periventricular crossroad areas correspond to the long axonal pathways connecting the cortex with the subcortical centers. They are particularly vulnerable to injury as their peak of growth is between 22 and 34 GW, exactly when PN are born.

Crossroad areas encompass hydrophilic extracellular matrix that contains axonal guidance molecules (Judas et al., 2005). Therefore, on T2w MRI they can be easily recognized as periventricular areas with high MR signal intensity.

Only the visibility of the five crossroad areas was assessed using coronal slices that were perpendicular to the AC-PC axial plane (Fig. 1):

- C1, the main frontal crossroad area, is located lateral to the lateral ventricle in the area where external and internal capsule converge (Fig. 1a).
- C2, another frontal crossroad area, is located just above the tip of lateral ventricle (Fig. 1a).
- C4, the parietal crossroad area, is located at the exit of the retro-ventricular portion of the posterior limb of the internal capsule (Fig. 1b)
- C5, the occipital crossroad area, is located dorsolateral to the posterior horn of the lateral ventricle, and in a proximity of parieto-occipital junction (Fig. 1c).
- C6, the temporal crossroad area, is located anterolateral to the tip of inferior horn of the lateral ventricle. The visibility of the C6 crossroad area has been assessed on the coronal plane passing through the amygdala (Fig. 1d).

We did not explore the crossroad area C3, which is located in frontal regions below the putamen and the caudate nucleus (Judas et al., 2005). C3 area is often below the MRI resolutions by its small size or mistaken for the olfactory migratory stream due to its proximity. Knowing that from 20–40 GW the periventricular crossroad areas are visible and can be distinguished from the surrounding tissue on *ex vivo*
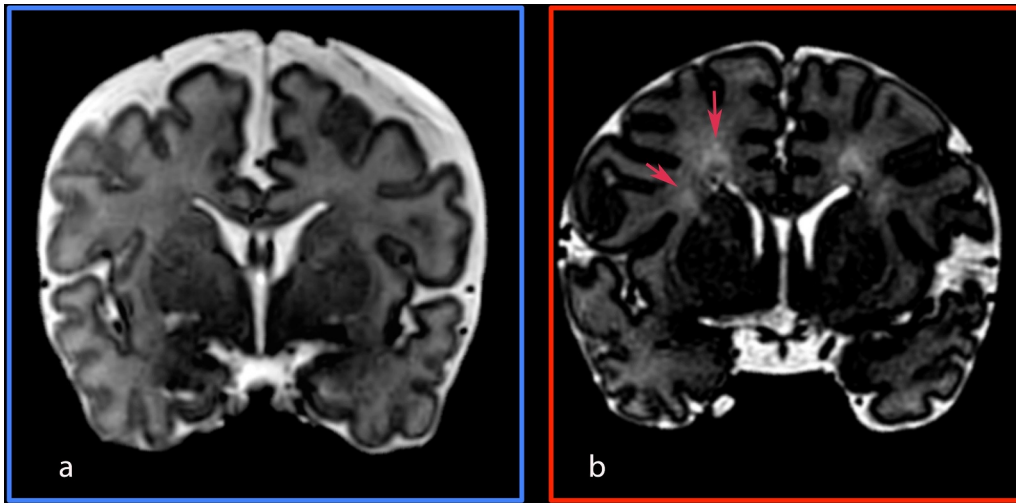
Fig. 2. Grading of periventricular crossroad areas on coronal T2w MR images. "Immature or dysmature" crossroad areas that are not visible (i.e. could not be distinguished from the surrounding tissue) have been assigned a value of 1 (**a**). Mature periventricular crossroad areas (red arrows in **b**) that are visible as focal hyperintensities on T2w MRIs have been assigned a value 2 (**b**).(For interpretation of the references to colour in this figure legend, the reader is referred to the web version of this article.)

MRI, we hypothesized that the crossroad areas that are visible on T2w MRI are mature. Thus, the crossroad areas that could be distinguished from the surrounding tissue have been assigned a grade level 2 (Fig. 2b). Contrarily, if the periventricular crossroad areas were not visible (i.e. could not be distinguished on T2w MRI from the surrounding WM tissue, which was also hyperintense), we referred to them as "immature", "dysmature", or "injured" and have assigned them a value 1 (Fig. 2a).

2.4.1.2. Von Monakow segments of the white matter. Towards the end of the gestation, fetal WM becomes organized, based on the descriptions of von Monakow (1905). This organization parallels the beginning of the myelination. Thus, on T2w MR images the compact fiber bundles that start to myelinate become hypointense compared to the more immature and unmyelinated WM. Consequently, the gradual radial myelination of axonal pathways, which pass through the von Monakow segments of WM (Kostovic et al., 2014) can be used for the gradation of the maturity level of these bundles. We hypothesized that more myelin leads to hypointense T2w MR signal intensity and corresponds to more mature WM. Contrarily, the hyperintense T2w MR signal intensity of the WM would reflect delayed maturation or dysmaturation of the particular segment. The T2w hyper- or hypo- intensity of von Monakow segment was visually assessed by comparing its T2w signal intensity to the T2w signal intensity of the surrounding WM. This was crucial as myelination and oligodendrocyte maturation follows a radial pattern from ventricles to the pia. The hyperintense T2w segment of WM, relative to its neighboring segments, was assigned a value of 1 (immature) (e.g. Figs. 3a, 4a, 5a). Hypointense T2w segment, compared to its neighboring WM, was assigned a value 2 (intermediate level of maturity, Figs. 3b, 4b, 5b). Finally, if a von Monakow segment of the WM was of moderate T2w MR signal intensity, and could not be distinguished from the surrounding WM, also of moderate T2w MR signal intensity, we assigned it a value 3 (mature) (e.g. Figs. 3a*, 3c*, 4c, 5c).

Coronal sections that were perpendicular to the AC-PC line were used for grading the maturity level of von Monakow segments of WM in frontal, central, and occipital regions.

- Von Monakow segment I (Fig. 3) is a periventricular compartment of fibers mainly composed of callosal radiation, associative fronto-occipital fascicle, motor cortico-striatal, and cortico-pontine pathways. They are particularly vulnerable in children born PN and their underdevelopment has been associated with cognitive deficit (Vasung, 2011). On coronal sections, perpendicular to the AC-PC line, in frontal (Fig. 3a, a*), central (Fig. 3b, b*), and parieto-occipital regions (Fig. 3c, c*) von Monakow segment I is located adjacent to the lateral ventricles.

- Von Monakow segment II (Fig. 4) is an intermediate compartment of the WM, a remnant of fetal intermediate zone. It is situated between the von Monakow segment I and von Monakow segment III (gyral WM). It contains periventricular crossroads and fibers radiating from the internal and the external capsule, which form the sagittal strata. Sagittal strata is most prominent in the occipital lobe and encompass projection from sensory thalamus and from motor cortex via thalamocortical and pyramidal tracts. On coronal sections, perpendicular to the AC-PC line, in frontal, central, and parieto-occipital regions, it is located below the center of the centrum semiovale.

- Von Monakow segment III (Fig. 5) corresponds to the developing centrum semiovale. The centrum semiovale is composed of long associative fiber systems (superior longitudinal fascicle, arcuate fascicle, inferior longitudinal fascicle), and the projection fibers. The proposed border between segment II and the segment III is the myelinated external capsule. On coronal sections, perpendicular to the AC-PC line, in frontal, central, and parieto-occipital regions von Monakow segment III is located within the center of the centrum semiovale.

2.4.1.3. Bands of migrating glial and neuronal cells. During the radial and tangential migration, glial and neuronal cells pass through the deep periventricular WM (Paredes et al., 2016). Thus, visibility of migrating cell bands were suggested to be related to the immature WM (Childs et al., 2001). The number of visible bands is reported to be inversely related to the gestational age. These bands disappear shortly after birth. If present at term age, the bands of migrating cells are located in the deep periventricular WM of the frontal lobe and have hypointense T2w MR signal intensity (Paredes et al., 2016). If they were visible, periventricular bands of migrating cells were assigned a value 1 (immature) (Fig. 6a), if no bands were identified they were assigned a value 2 (mature) (Fig. 6b).

2.4.2. . Grading the level of maturity of the subplate compartment

The transient subplate compartment is located between the von Monakow segment III and the cortical plate. It appears around the 10th GW and disappears between 3 and 12 postnatal months according to the brain region (Kostovic et al., 2002).

Before 34 GW the subplate compartment is characterized by a high T2w MR signal intensity (Rados et al., 2006; Vasung et al., 2016) and can be delineated as a continuous zone within the telencephalic wall. However, after 34 GW on T2w MRIs it has a patchy appearance i.e. the
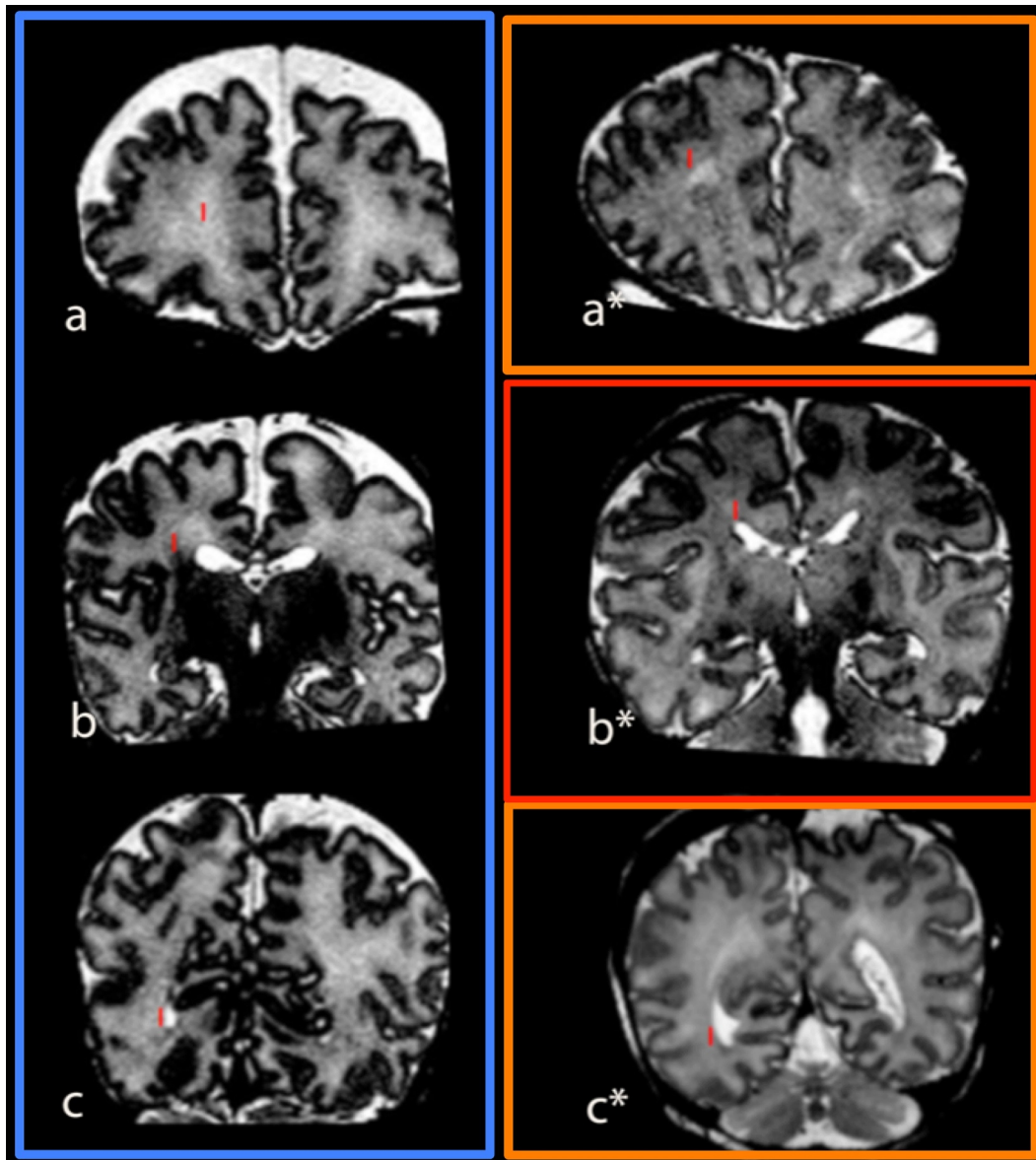
Fig. 3. Von Monakow white matter segment I. Von Monakow white matter segment I belongs to the deep periventricular fibers system. On coronal sections, perpendicular to the anterior commissure-posterior commissure line, von Monakow segment I that is hyperintense on T2w MRI, compared to the surrounding white matter was assigned a value 1 (immature) (**a, b, c, blue frame**). The von Monakow segment I that is hypointense on T2w MRI, compared to the surrounding white matter was assigned a value 2 (intermediate maturity level) (**b*, red frame**). The von Monakow segment I that has a moderate T2w MR signal intensity, and could not be distinguished from the surrounding WM, also of moderate T2w MR signal intensity, was assigned a value 3 (mature) (**a*and c*, orange frame).**(For interpretation of the references to colour in this figure legend, the reader is referred to the web version of this article.)

high T2w MR signal intensity areas are intermixed with the areas of moderate to low T2w MR signal intensities (Ivica and Judas, 2010). Around the term age, the reorganization of the cellular and the extracellular components of the subplate compartment leads to a transient, well-delineated, ribbon-like T2w hyperintensity, first seen in the central regions (from 36th GW), then in occipital regions (2 months), and finally in frontal regions (12 months) (Ivica and Judas, 2010). This ribbon-like pattern closely follows the contours of the cortical plate (Ivica et al., 2014b). The maturity of the subplate compartment was assessed on coronal sections, perpendicular to the AC-PC line, in frontal (Fig. 7a, d, g), central (Fig. 7b, e), and parieto-occipital regions (Fig. 7c, f, h). If the subplate compartment appeared "patchy" like hyperintensities within the gyri, we assigned it a value 1 (immature, red arrows in 7a, 7b, 7c). T2w hyperintense, ribbon-like subplate band, lining the gyral and sulcal cortical plate, was assigned a value 2 (i.e. intermediate level of maturity, red arrows in 7d, 7e, 7f). If the subplate

compartment was T2w hypointense in all the regions of the telencephalon, together with the hypointense white matter, it was assigned a value 3 (7g, 7h).

2.4.3. Grading the gray matter level of maturity
2.4.3.1. Gyrification level. Extensive cortical folding occurs mainly exutero for infants born preterm (Kostovic and Vasung, 2009) and may be disrupted by a preterm birth (Dubois et al., 2008a). To assess the level of the cortical gray matter maturity at TEA we have adopted a simple measure of gyral height to width ratio (van der Knaap et al., 1996). Using OsiriX® software we reconstructed the brain in 3D with axial sections parallel and passing through the AC-PC line, sagittal sections parallel or passing through the AC-PC line, and coronal sections that were perpendicular to the AC-PC line. Four gyri were assessed. Depending on the brain regions, we choose coronal sections or axial sections. Therefore, the gyrus of interest was cut perpendicularly and
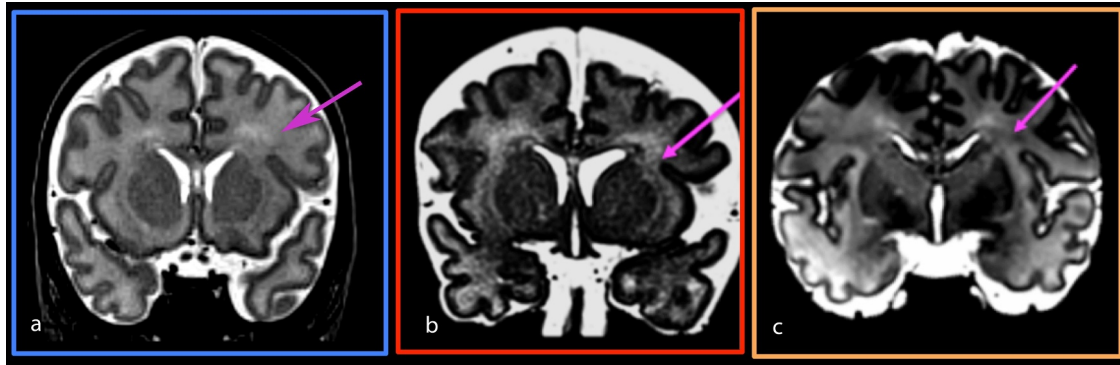
Fig. 4. Von Monakow white matter segment II in central area. The von Monakow white matter segment II largely overlaps with the remnants of the fetal intermediate zone. Thus, it contains fibers radiating from the internal and the external capsule as well as periventricular crossroads of growing axonal pathways. On coronal sections, perpendicular to the anterior commissure-posterior commissure line, von Monakow segment II is located between the periventricular white matter and white matter of the gyri, i.e. below the centrum semiovale. The von Monakow segment II that is hyperintense on T2w MRI, compared to the surrounding white matter, was assigned a value 1 (immature/dysmature) (**a, blue frame**). The von Monakow segment II that is hypointense on T2w MRI compared to the hyperintense surrounding white matter was assigned a value 2 (intermediate level of maturity) (**b, red frame**). Von Monakow segment II that has moderate T2w signal intensity, and cannot be distinguished from the surrounding white matter tissue, also of moderate T2w signal intensity, was assigned a value 3 (mature) (**c, orange frame**).(For interpretation of the references to colour in this figure legend, the reader is referred to the web version of this article.)

enabled a reliable measure of gyral height and width.

The gyral height and width of the superior frontal gyrus and medial frontal gyrus were measured on axial sections (Fig. 8a, b). The gyral height and width of the superior temporal gyrus (Fig. 8c, d) and superior parietal lobule were measured on coronal sections.

Cortical gyration was rated 1 (immature) if the depth of sulci was shorter than the width of gyri (Fig. 8a). If the depth of sulci was longer than the width of gyri (Fig. 8b, c, d) the gyration for this brain was rated as 2 (mature).

2.4.3.2. Germinal matrix. From mid-gestation onwards the germinal matrix, composed of tightly packed neuronal and glial precursors, decreases significantly in volume (Vasung et al., 2016). During the last few weeks of pregnancy, the germinal matrix is reduced to a tiny ventricular cellular lining. The last involution of the germinal matrix occurs near the term age in the roof of the temporal horns of the lateral ventricle (Fig. 9a), over the head of the caudate nucleus (Fig. 9b), and along the lateral wall of the occipital horn of the lateral ventricles (Fig. 9c). The germinal matrix is easily seen on T2w MRI as hypointense periventricular bands that are lining the ventricular walls (Paredes et al., 2016). If the germinal matrix was visible over the head of the caudate nucleus and the lateral walls of the occipital horn of the lateral ventricles they were assigned a value 1 (immature). In case the germinal matrix could not be identified, we have assigned this subject a value 2 (mature germinal matrix).

2.4.4. Grading the amount of the subarachnoid space

The width of the subarachnoid space gives indirect information about the brain volume. Its bulk is often more useful than the measurement of the head circumference (Armstrong et al., 2002; Horsch et al., 2005a; Shimony et al., 2016). The size of the subarachnoid space was determined by measuring the thickness of the subarachnoid space between the cortex and the skull in frontal and central regions. As the cerebral cortex is around 2 mm thick at term age (Vasung et al., 2016) visual impression of the thickness of the subarachnoid space, compared to cortex, provided the fastest assessment of its amount. Thus, if subarachnoid space was more than two times thicker than the cortex, it was larger than expected and we assigned to it a value 1 (Fig. 10a, a*). If its thickness was thinner than 4 mm (two times or less thicker than cortex) we have assigned to it a value 2 and interpreted normal width for term age (Fig. 10b, b*).
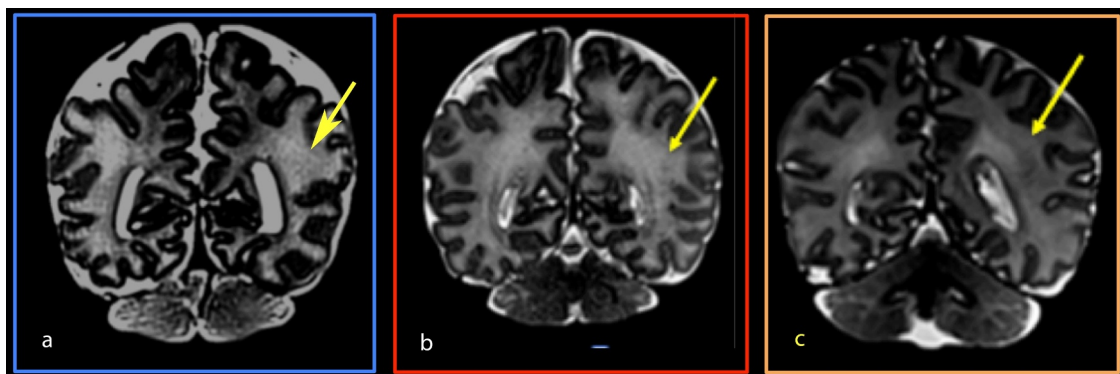

Fig. 5. Von Monakow white matter segment III. The von Monakow segment III of the white matter represents the developing centrum semiovale containing the long associative and projection fibers. It is located within the center of the centrum semiovale. On coronal sections, perpendicular to the anterior commissure-posterior commissure line, in this figure in parieto-occipital regions, von Monakow segment III is located just adjacent to the lateral ventricle. The von Monakow segment III that is hyperintense on T2w MRI and blended (cannot be distinguished) from the hyperintense surrounding white matter was assigned a value 1 (immature, **a, blue frame**). The von Monakow segment III that is hypointense on T2w MRI and surrounded by the hyperintense white matter was assigned a value 2 (intermediate maturity, **b, red frame**). The von Monakow segment III that is of intermediate T2w MR signal intensity and cannot be distinguished from the surrounding white matter tissue, also of moderate T2w signal intensity, was assigned a value 3 (mature), (**c, orange frame**).(For interpretation of the references to colour in this figure legend, the reader is referred to the web version of this article.)
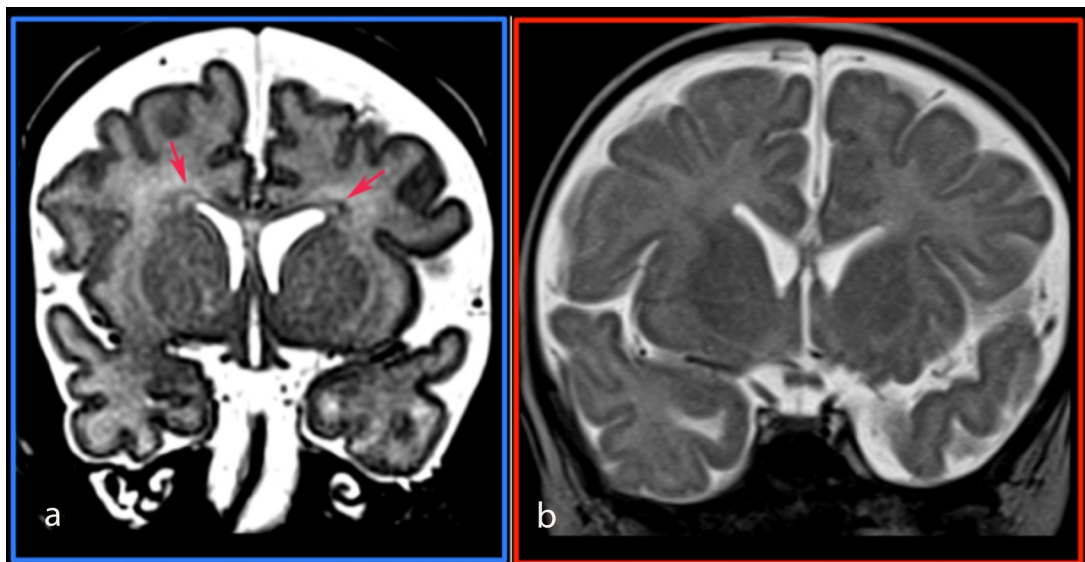
Fig. 6. Bands of migrating glial and neuronal cells. Bands of low T2w signal intensity in the deep periventricular regions of the frontal lobe (arrows in **a**) indicate ongoing migration of neuronal cells. We assigned value 1 (immature) if bands of low signal intensity can be seen in the frontal periventricular white matter. If the bands of migrating cells were not visible (**b**) we assigned a value 2 (mature).
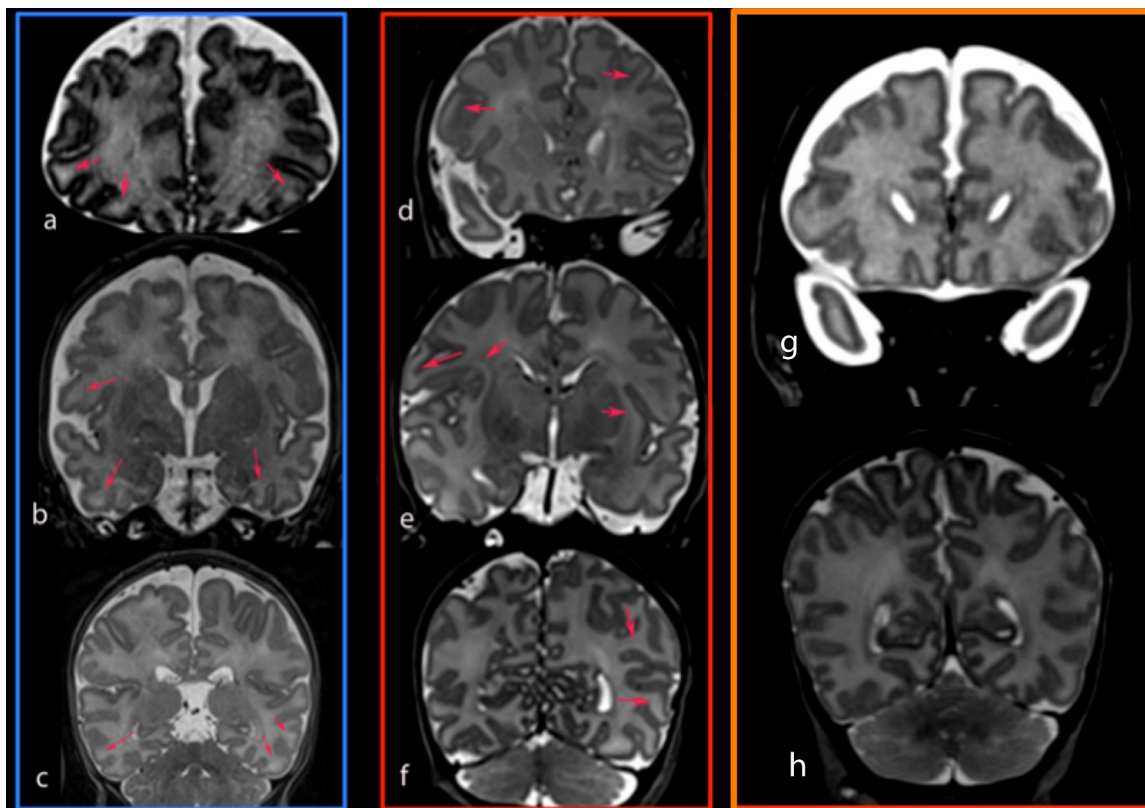
Fig. 7. Description of the subplate compartment. Subplate compartment can be visualized on coronal T2w MR images in frontal (coronal section passing the anterior part of the thalamus, **a, d**), central (coronal section passing the middle of the thalamus), and parieto-occipital regions (coronal section passing the posterior part of the thalamus **c, f**). Subplate appearance with "patchy" like hyperintensities within the gyri was assigned a value 1 (immature, **red arrows in a, b, c**). T2w hyperintense, ribbon-like subplate band, lining the gyral and sulcal cortical plate, was assigned a value 2 (mature, **red arrows in d, e, f**). In some rare cases, the subplate pattern is completely mature (score 3): no subplate is visible in frontal (**g**) and occipital (**h**). In some cases, the subplate pattern is completely mature (score 3): no subplate is visible in frontal (**g**) and occipital (**h**).(For interpretation of the references to colour in this figure legend, the reader is referred to the web version of this article.)

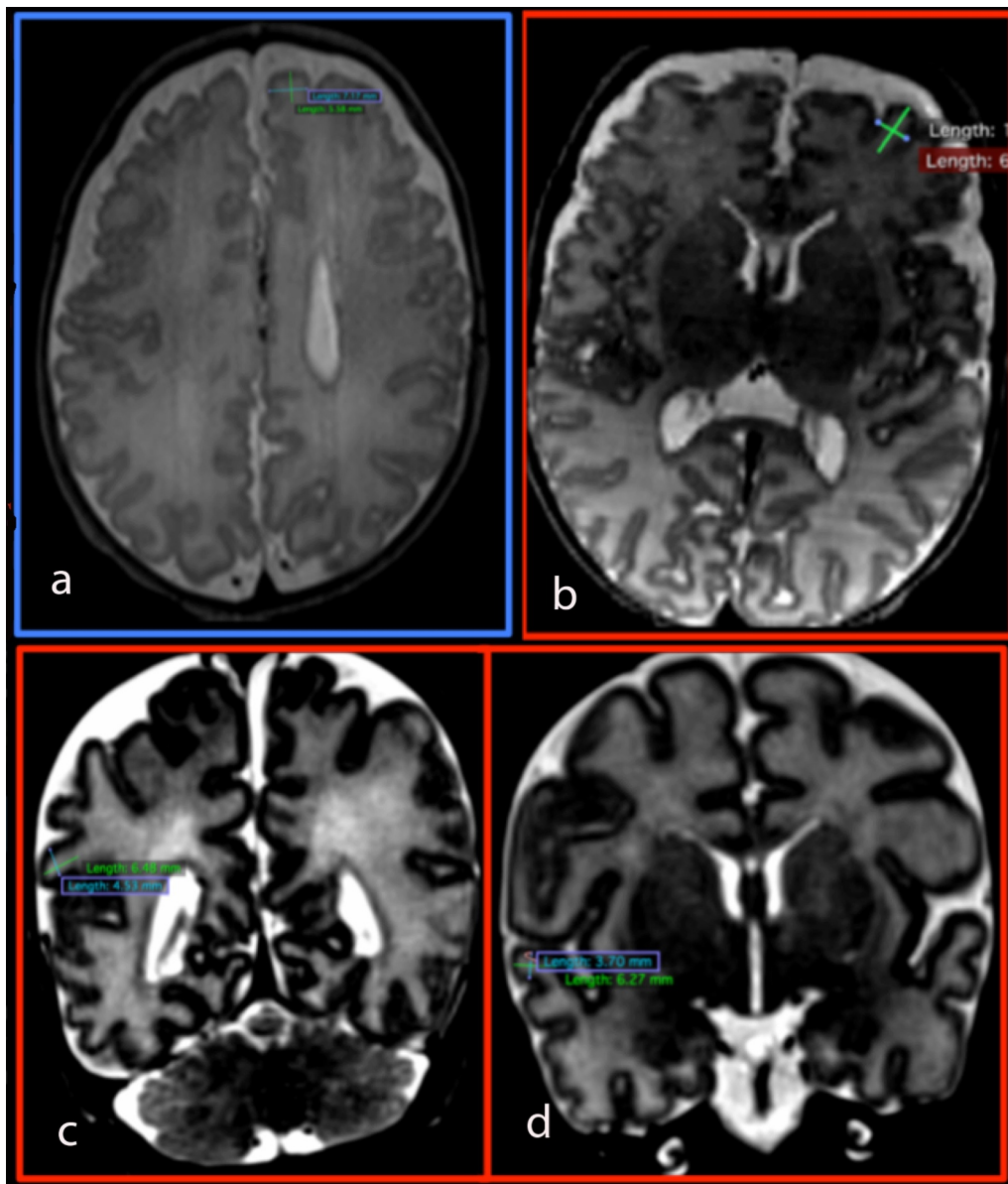**Fig. 8.** Grading the level of gyrification. Axial slices used to measure the height and the width of the superior frontal gyrus are shown in **a** and **b**. Coronal slices, perpendicular to the AC-PC line, were used to measure the width and the height of the posterior portion of the superior temporal gyrus (**c, d**). When the width of the gyri measured more than depth of the sulci the level of the gyrification was assigned a value 1 (immature), (**a, c**). When the depth of the sulci measured more than the width of the gyri the level of gyrification for that region of the brain was assigned a value 2 (mature), (**b, d**).

2.5. Statistical analyses

Statistical analysis was performed using Stata statistical 14.0 software (StataCorp, College Station, Texas).

The mean and standard deviation (SD) were used to for the continuous variable, while frequencies were used for categorical variables. Each MRI structure was analyzed separately. Mann-Whiney test or mean difference and 95% interval confidence were used when continuous variables were compared between two groups. X^2 tests or Fisher's exact tests (in the case of small cell sizes) were used with categorical variables. Two-tailed P values < 0.05 were used to indicate statistical significance.

Interobserver reliability was assessed using the intraclass correlation coefficient (ICC) (Groppo et al.) for continuous variables, and the Fleiss' Kappa for categorical variable by three raters. Kappa coefficients were also used to measure intra-observer reliability with 95% confidence intervals. We interpreted the kappa values as described by

Landis and Koch (1977). Kappa values < 0 indicated no agreement, 0–0.20 slight, 0.21–0.40 fair, 0.41–0.60 moderate, 0.61–0.80 substantial, and 0.81–1 almost perfect agreement.

3. Results

3.1. Patient population

T2w MRI images of 41 PN and 21 TN subjects were read. Demographic data are summarized in the Table 1. At the time of the MRI scan, the PN group was in mean 2.8 days younger (95%CI 0.06 to 0.7) compared to the TN group.

3.2. Inter- and intra-rater reliability

Inter-rater reliability for MRI is presented in the Table 2. The inter-rater agreement between the three readers ranged from moderate to

Fig. 9. Germinal matrix. At term age, germinal matrix can appear as T2w MRI hypointense proliferative zones in the roof of the temporal horn of the lateral ventricle (arrow in **a**), over the head of the caudate nucleus (arrow in **b**), and along the lateral wall of the occipital horn (arrow in **c**). If the germinal matrix was visible over the head of the caudate nucleus and along the lateral wall of the occipital horn we have assigned a value 1 (immature). If no germinal matrix was visible, we have assigned a value 2 (mature).

excellent. All three readers agreed almost perfectly in the scoring of the crossroads (Kappa coefficient between 0.86 and 1). The ICC for the interrater agreement was substantial for grading the maturity level of von Monakow segment I (ICC 0.7, 95% CI 0.6-0.8), von Monakow segment III (ICC 0.8, 95% CI 0.72-0.87), and the maturity level of the subplate (ICC 0.79, 95% CI 0.7-0.86). The ICC was moderate for the grading of maturity level of von Monakow segment II (ICC 0.6, 95% CI 0.46-0.72), excellent for the assessment of subarachnoid space thickness (ICC 0.9, 95% CI 0.84-0.93), and substantial for the degree of cortical folding (ICC 0.64, 95%CI 0.47-0.77). Considering the scoring of
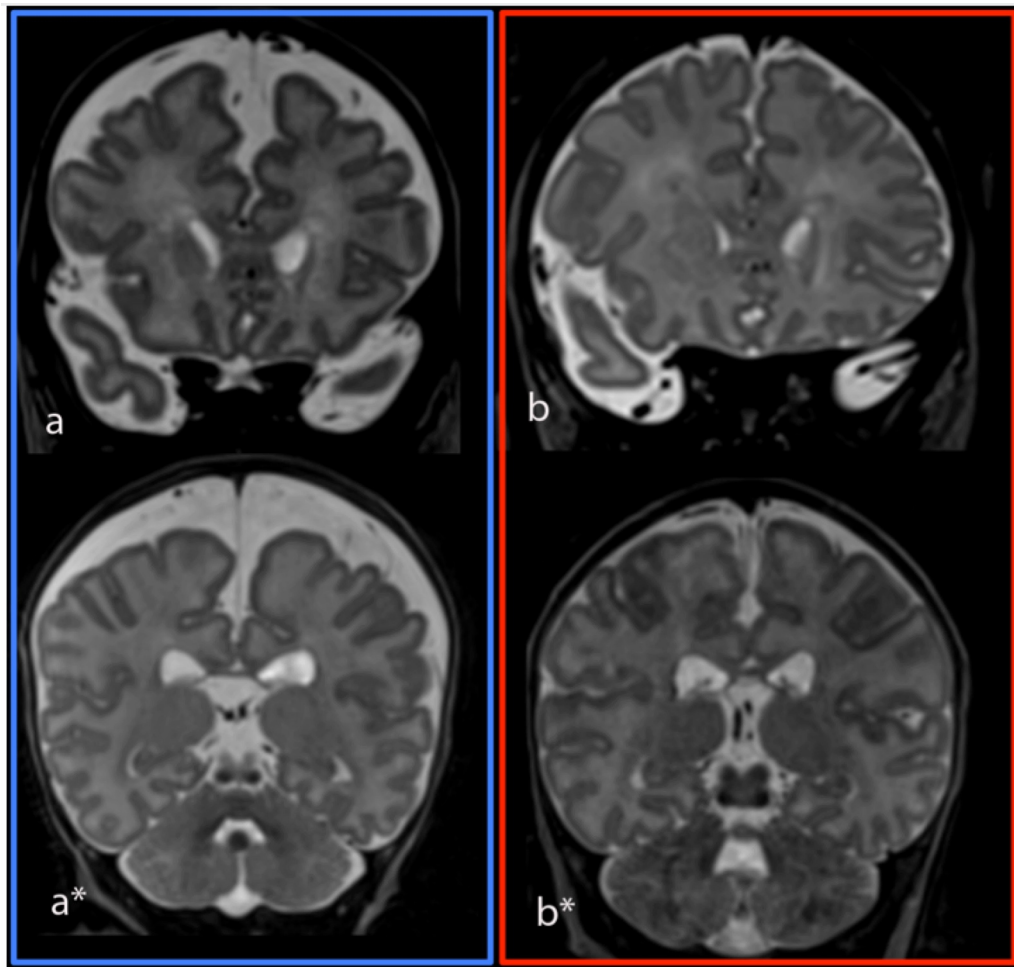
Fig. 10. Grading the amount of the subarachnoid space. Coronal T2 w MRI in frontal (**a, b**) and central (**a*, b***) regions. If subarachnoid space was > 2 times thicker (> 4 mm) than the underlying cortical plate, we assigned a value 1 for each region (immature), (**a, a***). If the subarachnoid space was ≤ 2 times of the thickness (≤ 2 mm) of the underlying cortical plate, we assigned a value 2 for each region (mature), (**b, b***).

Table 1
Characteristics of the term born and preterm born groups at the time of the MRI.

	Term-born infants n = 21	Preterm infants n = 41	*p-value*
Gestational age, in weeks	40.1, SD 0.6 (39.1 – 41.3)	28.3, SD 1.9 (25 – 33)	N.A.
Birth weight < 2 SD	0	4 (10%)	0.3
Male	21 (52%)	16 (39%)	0.4
Cranial circumference < 2 SD	0	9 (22%)	**0.02**
Multiple birth	0	14 (34%)	**0.001**
Antenatal corticosteroids	N.A.	31/41 (76%)	
Bronchopulmonary dysplasia			
-mild	N.A.	9/41 (22%)	
-moderate	N.A.	6/41 (15%)	
-severe	N.A.	1/41 (2.4%)	
Persistent ductus arteriosus			
-medical treatment	N.A.	8/41 (20%)	
-chirurgical treatment	N.A.	3/41 (7%)	
Confirmed sepsis	N.A.	6/41 (15%)	
Necrotizing enterocolitis	N.A.	1/41 (2%)	
Postmenstrual age at MRI, in weeks	40.5, SD 0.6 (39.4 – 41.5)	40.1, SD 0.6 (38.9 – 41.4)	**0.03**

Data are presented as either n (%) or mean, standard deviation (maximum value – minimum values). Difference between groups for continuous variables was calculated using the Mann-Whitney test. For comparison of categorical or binary outcomes between groups we used fisher or chi2 tests.
Note: N.A., not applicable; NEC, necrotizing enterocolitis; SD, standard deviation.

germinal matrix and bands of migration cells visibility, the agreement between the three raters was good (Cohen's Kappa coefficient of 0.67, 95% CI 0.47 - 0.77 and 0.79, 95% CI 0.5 - 0.8 respectively).

Intra-rater agreement was good to excellent for majority of anatomical structures. However, it was moderate to substantial for the crossroads 2, moderate for von Monakow segment III, and slight to fair for von Monakow segment II (Table 2).

3.3. Transient fetal structures and the brain maturity grade in term born infants

Table 3 summarizes the maturational level expected for each item in healthy TN, considered as the reference group. These expected maturational levels were deduced from their prevalence as shown in Supplementary Table 1, which gives detailed scoring for each structure for each reader. A cumulative score of 43 is expected at term age. The

mean cumulative maturity score in TN group was 41 (SD 1.4). Although several TN infants had the same cumulative score, no one had the same maturational pattern between the different structures as demonstrated in Graph 1.

The WM in TN is still maturing. All crossroads were visible as areas of high T2w MR signal intensity (mature). However, none of the von Monakow segments was found to be mature. Contrarily to the WM, gray matter in TN was well-developed with complex cortical gyrification in frontal, parietal and temporal regions. However, majority of TN had visible germinal matrix. The subplate compartment was visible in almost all subjects as a T2w hyperintense ribbon like zone lining the cortical plate in frontal, central, and occipital regions. However, 30% of TN had immature subplate compartment in fontal regions (Supplementary Table 1). All TN except one had thin subarachnoid space in frontal and parietal regions (Supplementary Table 1).

3.4. Transient fetal structures and the brain maturity grade in preterm born infants at TEA

As represented in Table 3 we could not map a common maturational stage of the fetal transient compartments in TEA-PN group. The level of maturity of crossroads 1, von Monakow segment II central, von Monakow segment III frontal was ambiguous. Indeed, for these structures, values 1 and 2 were assigned in similar proportions in TEA-PN group (Supplementary Table 1).

The mean cumulative score for TEA-PN group was 37 (SD 2.5). As shown on Graph 1, each TEA-PN subject had his own maturational pattern. Mature and less mature structures could coexist in the same TEA-PN subject.

3.5. Comparison of maturity score between term born infants at premature infants at TEA

Compared to TN group (41, SD 1.4), the mean global scores in TEA-PN group (37, SD 2.5) were significantly lower (i.e. lower level of maturity, p < 0.001). At TEA, former PN scored globally 0.5 points less per each week of prematurity (coefficient 0.5, 95% IC 0.4 – 0.8). The gradual changes in maturity level per subject from lower to higher gestational age at birth can be appreciated in the Graph 1. The most discriminatory brain structures between both groups were the following structures: crossroads 1 and 4, von Monakow segments III central, occipital and the subplate compartment frontal and occipital. For the parameters used in prior scoring systems, frontal gyrification and subarachnoid space were also discriminatory structures. Supplementary

Table 2
Intra- and inter-rater agreement of each structure read on MRI.

	Inter-rater realibility Reader 1, Reader 2, Reader 3 ICC	Intra-rater realibity Reader 2 ICC or Kappa	Intra-rater realibity Reader 3 ICC or Kappa
Crossroads			
Crossroad area 1	0.92 95%CI (0.88 – 0.95)	K 1.00 (p 0.001)	K 0.91 (p 0.001)
Crossroad area 2	0.94 95%CI (0.9 – 0.95)	K 0.47 (p 0.005)	K 0.65 (p 0.001)
Crossroad area 4	0.94 95%CI (0.9 – 0.95)	K 1.00 (p 0.001)	K 1.00 (p 0.001)
Crossroad area 5	1.00	K 1.00 (p 0.001)	K 1.00 (p 0.001)
Crossroad area 6	0.86 95%CI (0.8 – 0.9)	K 0.72 (p 0.001)	K 0.7 (p 0.001)
Von Monakow segment I	ICC 0.7 95%CI (0.6 – 0.8)	ICC 0.88 95CI (0.75-0.93)	ICC 0.93 (0.85-0.96)
Von Monakow segment II	ICC 0.6 95%CI (0.46 – 0.72)	**ICC 0.2 (-0.16 – 0.5)**	ICC 0.36 (0.4 – 0.62)
Von Monakow segment III	ICC 0.8 95%CI (0.72 -0.87)	ICC 0.56 (0.27 – 0.76)	ICC 0.82 (0.65 – 0.9)
Bands of migration	ICC 0.79 95%CI (0.7 – 0.86)	K 1.00 (0.001)	K 1.00 (0.001)
Gyrification with deep sulci	ICC 0.64, 95%CI (0.47-0.77)	K 0.92	K 0.91
Germinal matrix	ICC 0.67 95%CI (0.5 – 0.8)	K 1.00 (0.001)	K 1.00 (0.001)
Subplate compartment	ICC 0.79, 95% CI (0.7 – 0.86)	ICC 0.9 (0.82 – 0.95)	ICC 0.91 (0.83 – 0.97)
Subarachnoid space < 4 mm	ICC 0.9, 95%CI (0.84-0.93)	K 0.97	K 0.94

Note: K, Kappa coefficient ; ICC, interclass correlation coefficient.
Values < 0 as indicating no agreement, 0 – 0.20 as slight, 0.21 – 0.40 as fair, 0.41 – 0.60 as moderate, 0.61 – 0.80 as substantial, and 0.81 – 1 as almost perfect agreement.

Table 3

In bold, maturational states of the important fetal transient compartments still expected to be seen at birth in term group considered as reference and in preterm group at term equivalent age. To give a global vision of our scoring system, we introduced the quality of the gyrification and the visual aspect of subarachnoid space. Regular numbers are, for each structure, the highest possible scores and represent a mature state.

	Term infants	Preterm infants at term equivalent age
White matter and subplate compartment		
Crossroads		
C1	mature (score **2**/2)	**ambiguous between score 1vs 2**
C2	mature (score **2**/2)	mature (score **2**/2)
C4	mature (score **2**/2)	**immature (**score **1**/2)
C5	mature (score **2**/2)	mature (score **2**/2)
C6	mature (score **2**/2)	mature (score **2**/2)
Expected sum	**10**/10	
Von Monakow segment I		
frontal	**probably immature (score 1**/3)	**immature (score 1**/3)
central	on maturing (score **2**/3)	on maturing (score **2**/3)
occipital	on maturing (score **2**/3)	on maturing (score **2**/3)
segment II		
frontal	immature (score **1**/3)	immature (score **1**/3)
central*	on maturing (score **2**/3)	**ambiguous between score 1 vs 2**
occipital	immature (score **1**/3)	immature (score **1**/3)
segment III		
frontal	on maturing (score **2**/3)	**ambiguous between score 1 vs 2**
central	on maturing (score **2**/3)	on maturing (score **2**/3)
occipital	on maturing (score **2**/3)	**immature (score 1**/3)
Expected sum	**15**/27	
Subplate compartment		
frontal	on maturing (score **2**/3)	**immature (score 1**/2)
central	on maturing (score **2**/3)	on maturing (score **2**/3)
occipital	on maturing (score **2**/3)	**immature (score 1**/2)
Expected sum	**6**/9	
Bands of migration	immature (score **1**/2)	immature (score **1**/2)
Expected sum	**1**/2	
Maturity score of white matter components	**32**/47	
Gray matter		
Gyrification		
frontal	well-developed (score **2**/2)	**ambiguous**
temporal	well-developed (score **2**/2)	well-developed (score **2**/2)
parieto-occipital	well-developed (score **2**/2)	well-developed (score **2**/2)
Expected sum	**6**/6	
Germinal matrix		
Expected sum	immature (score **1**/2)	immature (score **1**/2)
	1/2	
Subarachnoid space		
frontal		
parietal	thin (score **2**/2)	**thick (score 1**/2)
Expected sum	thin (score **2**/2)	thin (score **2**/2)
	4/4	
Maturity score of gray matter components	**11**/12	
Cumulative maturity score expected at term age	**43**/60	

Note: vs, versus.

table 1 shows the prevalence of the different maturity levels of the transient fetal brain structures as seen on T2w MRI between TN and TEA-PN groups and their statistic between both neonatal populations. Crossroad 1 areas were visible in >90% of TN while they were seen only in 60 % of PN babies at TEA. The crossroads 4 were visible in 80% of the TN but only in 20% of PN babies at TEA. Mann-Whiney test revealed that scores given to von Monakow segment III in occipital regions, subplate compartment in frontal and occipital regions, and subarachnoid space in frontal regions were significantly smaller in PN at TEA compared to TN for all three readers (p < 0.002) (Supplementary Table 1). Therefore, our scores indicate that the maturation of the WM in PN at TEA affect the regions that are the most distant from the central subcortical structures (occipital and frontal regions) and from the ventricles (WM that is closer to the pial surface) (Fig. 11).

The frontal gyrification was still poorly developed in around half of PN at TEA, but only in 15% of TN. A similar pattern was observed for the subarachnoid space assessment. The frontal and parietal subarachnoid space was thin in almost all TN (100% and 95% respectively), while 70% of PN had thicker frontal subarachnoid space compared to the underlying cortex, with half of them having parietal subarachnoid space thicker than underlying cortex.

Subplate remnants with a "patchy" appearance (score 1, immature) were visible in a considerable proportion of PN in the frontal (80-95%) and occipital regions (60%) compared to a smaller number of subjects in the TN group (35% and 15% respectively).

If a majority of TEA-PN infants scored lower for most of brain structures, a higher proportion of TEA-PN (20%) have started to myelinate the von Monakow segment II of WM in its occipital regions compared to only 5% of the TN infants. In the same direction, value 3, which meant fully mature structure, was never given to TN but occasionally allowed to TEA-PN by one reader for von Monakow segments II and III in their frontal brain region and for subplate compartment in their frontal and occipital regions.

4. Discussion

In this study we propose a new MRI scoring system to assess the brain maturity in the newborns at term age. We hypothesized that the development of such a MRI scoring system based on prenatal ex vivo MRI and histological descriptions would be a solid source to assess the
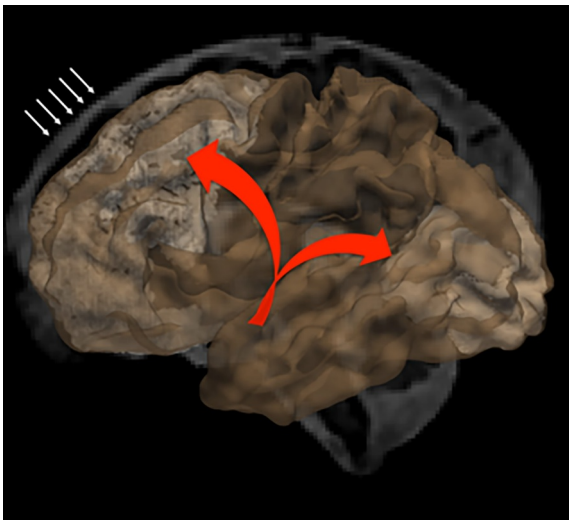
Fig. 11. Illustration of the significant results relevant for the assessment of the brain maturity level in TN and PN at TEA. Red arrows indicate the direction of the white matter (von Monakow segments of the white matter) and subplate maturation during the last trimester. The proposed maturation scheme is based on our results. Note the direction from the central regions toward the frontal and occipital lobe, and from the ventricles towards the pial surface. White areas in the frontal and occipital lobe indicate regions where superficial white matter (von Monakow segment III in the occipital lobe), and subplate compartment (in the frontal and occipital lobe) were found to be immature (dysmature) in the PN compared to the TN at TEA. Finally, PT, compared to the TN, had significantly thicker subarachnoid space in the frontal regions (white arrows).(For interpretation of the references to colour in this figure legend, the reader is referred to the web version of this article.)

maturity level of the white matter, gray matter, and subplate regions, known to be different in TN compared to PN (Horsch et al., 2005b). Thus, the neuroradiological criteria used in this current work were based on the description of fetal structures in studies using *ex vivo* MRI and histology (Judas et al., 2005; Kostovic et al., 2014).

We first demonstrate that the transient fetal structures such as crossroads, subplate compartment, and von Monakow segments of white matter can be identified reliably on the T2w MRI by clinicians (radiologist and paediatrician) with little or no previous training in fetal MR imaging. Inter-rater agreement and reliability between the three readers were more than satisfying for the MR identification of these transient fetal structures.

Next, the level of maturity for the components of the white matter, gray matter, subplate compartment, and subarachnoid space was compared between both TN and PN groups.

Our results indicate that the superficial regions of the WM (von Monakow segment III) and subplate zone are significantly different in PN at TEA compared to TN. We use here the term "immature". This term was the consensus between the clinicians involved in this study, as no brain injury was identified in our studied population. In the next few paragraphs we discuss the biological substrate that might underlie the 'immaturity' of the WM and the subplate compartment in PN at TEA. Finally, we acknowledge that the different T2w MR findings in PN might be caused by oligodendrocyte dysmaturation in WM (Back and Miller, 2014).

4.1. Global cumulative maturity scores

Our mean cumulative maturity scores distinguished PN at TEA from TN. On average, TEA-PN group scored 4 points (37, SD 2.5) lower than TN group (41, SD 1.4). PN infants scored 0.5 points lower per week of prematurity. The higher standard deviation in TEA-PN group showed that this population had a higher variability in their maturity pattern

than TN infants. These results suggest that the maturation of the brain during the postnatal life is a dynamic process and that the gestational age should be taken into account when assessing the maturity of the brain in PN at TEA.
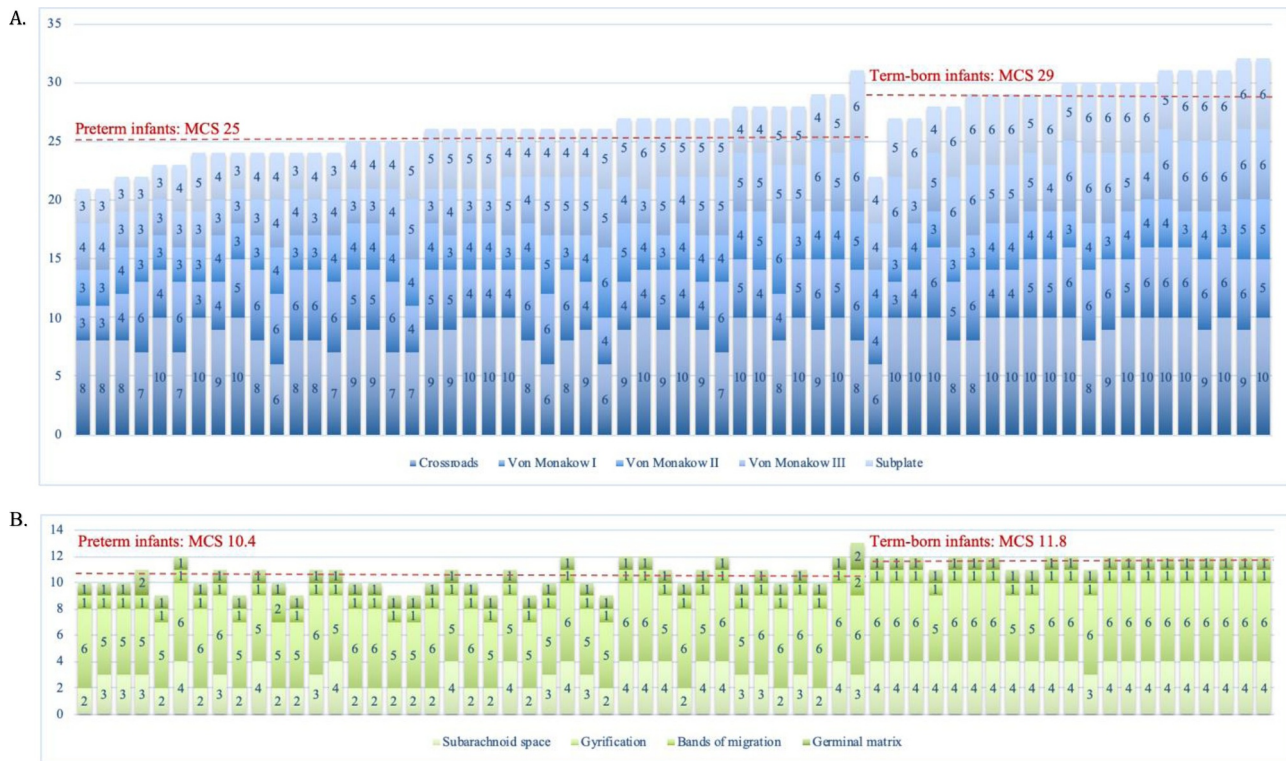
4.2. Maturation of the gray matter

The level of gyrification is a known biomarker of the gray matter maturation, and has been reported to be decreased in PN at TEA (Dubois et al., 2008b). Our paper confirms that the assessment of frontal gyrification provides a good discriminatory tool between PN at TEA and TN. In addition, germinal matrix can be reliably identified on T2w MRIs in a majority of subjects, independently of their belonging groups. Thus, the presence of germinal matrix did not discriminate PN at TEA from TN. In agreement with the recently described massive migration of neurons in the frontal lobe of the newborns (Paredes et al., 2016), our findings indicate that some neurogenesis and gliogenesis is still occurring at term age.

4.3. Maturation of the white matter

The most relevant differences between PN at TEA and TN were found in the WM maturation. As expected, PN at TEA and TN had immature WM. Indeed, T2w MR signal intensity across the WM was not uniform and none of the subjects reached the maximal score based on the T2w MR characteristics of the WM in the adult brain. In both neonatal groups, all von Monakow segments of the WM, which are radially arranged from ventricles to the pia, were of intermediate maturity in the central regions. Radiologically, the three von Monakow segments of the WM appeared in their central areas hypointense on T2w MRI and could be distinguished from each other. The intermediate WM segment (von Monakow segment II) was hyperintense and so considered as immature in the frontal and the occipital regions in PN at TEA and TN. These results are well in line with the known establishment of projection fibers connecting the subcortical structures to the cortical neurons at around 26 GW (Krsnik et al., 2017), followed by the early myelination (Yakovlev et al., 1967), seen as decreased in T2WI intensity (Barkovich et al., 1988).

The deep segments of the WM (von Monakow segment I, close to the ventricles) and intermediate segment of the WM (von Monakow segment II) were still immature (higher T2w MR signal intensity) in the frontal regions in both groups. Our results highlight that the maturation of von Monakow segments of WM in central regions precedes the maturation of von Monakow segments in frontal and occipital regions. In the frontal regions, the cellular migration and the growth of association fibres start during fetal period and extend into the newborn period (Dubois et al., 2008c; Paredes et al., 2016; Vasung et al., 2017). As the immature WM appears as T2w MRI hyperintensity due to higher content of extracellular matrix and water, we hypothesized that the immaturity of the deeper segments of the WM in the frontal regions causes a squishy environment and facilitates the migration of neurons and glia in the frontal lobe. Indeed, as already mentioned, we found that both neonate groups had visible bands of migrating cells in the frontal lobes. Compared to TN, PN infants at TEA showed an identical pattern of WM maturation (myelinization first in central areas, then in frontal and occipital regions) but with some delay except in the occipital regions of von Monakow segment II of the WM. Indeed, a substantial portion (20%) of PN at TEA had already started to myelinate the von Monakow segment II of WM in occipital regions compared to a minim portion (5%) of TN. These qualitative results could indicate a well-known accelerated maturation of the optic radiation upon a premature exposure to visual stimuli (Groppo et al., 2014). The optic radiation is located in the occipital part of von Monakow segment II of WM. On the other hand, 20-30% as many as TEA-PN had a less mature aspect of von Monakow segment III in frontal regions compared to TN. This finding might correspond to a protracted or perturbed development of long

A.

Term-born infants: MCS 29

Preterm infants: MCS 25

▪ Crossroads ▪ Von Monakow I ▪ Von Monakow II ▪ Von Monakow III ▪ Subplate

B.

Preterm infants: MCS 10.4

Term-born infants: MCS 11.8

▪ Subarachnoid space ▪ Gyrification ▪ Bands of migration ▪ Germinal matrix

Graph 1. Repartition of the maturity level per subject for each brain structure. **A.** The newly proposed brain structures: crossroads, the 3 von Monakow segments, the subplate compartment. **B.** the brain structures previously described as different in preterm infants at term equivalent compared to term-born infants: gyrification, bands of migrating cells, germinal matrix, and subarachnoid space. Gestational age at birth is plotted on the X-axis. Y-axis shows the estimated maturity level for each subject. Each column represents one subject. The brain structures are color coded. Numbers are the median scores given by the 3 raters. For clarity purposes, the median scores of a particular brain structure are summed together. For example, the median scores of all 5 crossroads were summed together and reported as one number. Higher numbers indicate a more mature stage. The maximal possible score is different from one region to another. Maximal/minimal possible score per structure: crossroads areas 10/5, von Monakow segment I 6/3, von Monakow segment II, III 9/3, subplate compartment 9/3, subarachnoid space 4/2, gyrification 6/3, bands of migrating cells 2/1, germinal matrix 2/1. The red dotted line is the mean cumulative score (MCS) given separately in term and preterm infants at term equivalent age.

associative cortico-cortical tracts, which belong to von Monakow III segment, in frontal regions in prematurely born infants. It is likely that the dysmaturation of the oligodendrocyte precursors in different segments of WM (from ventricles to pia) is determined by the timing of the birth and the localization of oligodendrocytes at this given time (Haynes et al., 2013; Kinney, 2006; Kinney et al., 2012; Volpe et al., 2011). A premature exposure to the environment might affect the re-organization of the WM and leads to its dysmaturation, especially in the superficial von Monakow segment III of the frontal and occipital regions. As also mentioned by Allin and al. (Allin et al., 2011) our results suggest a different growth of WM in PN with both delayed and accelerated maturation. It could be assumed that advanced maturation processes are affecting critical period maturation and therefore would not provide longterm benefit (Ivica et al., 2011). Further studies confronting the maturation level of transient fetal brain structures with later neurodevelopmental outcome (Fischi Gomez et al., 2015; Karolis et al., 2017) must be performed to investigate if our findings can mirror later neurodevelopment and be valuable for counselling.

On T2w MRI the majority of TN and PN at TEA had all crossroads visible as periventricular areas of high signal intensity T2WI (Kostovic and Vasung, 2009). However, we found, that crossroads C1 and C4 were good discriminatory items between TN and TEA PN. Indeed, a significant portion of PN at TEA had their crossroad C1 and C4 areas indistinguishable from surrounding WM. The tendency of PN at TEA to have "immature" C1 and C4 crossroad areas might be associated with the WM immaturity/dysmaturity of PN at TEA reported by Back (Back and Miller, 2014). Corticospinal, thalamocortical, callosal, fronto-occipital and fronto-pontine pathways pass through the C1

periventricular crossroad area, while geniculocortical projection, callosal fibers, and associative corticocortical fibers pass through the C4 crossroad area (Vasung et al., 2011; Vasung et al., 2010). Periventricular crossroads C1 and C4 are situated in the regions that are commonly injured in the PN (Volpe, 2009). Thus, it might be possible that these injured or dysmature crossroad areas through which the association, projection, and callosal fibers cross, are a biological substrate of the long-term complex adverse outcomes of prematurity (Fischi Gomez et al., 2015).

4.4. Maturation of the subplate compartment

Subplate compartment is a transient fetal compartment that can be identified on T2w MRI of fetuses as early as 17 GW (Rados et al., 2002). During the fetal and early preterm periods (<30 GW) on T2W MRI (Khan et al., 2019) the subplate compartment is visible as a continuous zone of high signal intensity. Around 30 GW the reorganization and resolution of the subplate zone start. The subplate zone appears as "patchy". Areas of high T2w MR signal intensity are seen in the crowns of gyri with areas of low T2w MR signal intensity beneath the sulci. Towards the first postnatal month the "patchy" appearance of the subplate zone is replaced by a ribbon-like T2w hyperintense appearance (for detail descriptions of the subplate reorganization see Kostovic et al., 2014). High T2w MR signal intensity of the subplate zone has been contributed to its rich content of extracellular matrix molecules that guide axons towards their final destination in the cortical plate (Kostovic et al., 2011). The transition from "patchy" to ribbon-like subplate appearance coincides with the relocation of the

short cortico-cortical axons from the subplate compartment to the cortical plate (Kostovic et al., 2014). The timing of this axonal relocation varies from region to region (Krsnik et al., 2017).

In majority of TN the subplate compartment of frontal, central, and occipital regions had a T2 hyperintense, ribbon-like appearance, interpreted as an intermediate level of maturity as the subplate compartment was still visible. Compared to the TN infants, a significant proportion of PN at TEA have still a patchy and immature appearance of the subplate compartment in the frontal and occipital regions. Thus, PN at TEA have most likely protracted or altered relocation of axonal fibers from subplate to cortical plate in frontal and occipital regions. This discovery is in line with several previous studies, which showed that dysmaturation changes in the WM, seen after a premature birth, persist into childhood (Ball et al., 2012; Ball et al., 2015; Fischi Gomez et al., 2015; Volpe, 2009).

In conclusion, our results indicate that the reorganization of the subplate compartment in frontal and occipital regions is different in PN compared to the TN at TEA.

4.5. Subarachnoid space and cerebrospinal fluid

Compared to the TN, TEA-PN had a higher amount of subarachnoid space occupied by the cerebrospinal fluid. As micro-vessels are of crucial importance for the regulation of interstitial fluid and cerebrospinal fluid volume (Oreskovic and Klarica, 2011), our findings suggest that the auto-regulation of the cerebral blood vessels might be different in prematurely born infants. However, this hypothesis remains to be confirmed. In addition, the thicker subarachnoid space in the frontal regions might indirectly indicate an altered development leading to the smaller volumes of the frontal lobe.

4.6. Limitations

Study limitations include the small size of our cohort which decreases the power for variables with low prevalence. Studies with larger population are needed to validate our findings and allow generalization. A second limitation is the slight to fair intra-rater rate for the von Monakow of WM segment II. However, moderate inter-rater reliability supports our results. The low inter-rater reliability pointed out the difficulties in scoring this structure. Consequently, we are exploring a different approach to identify and score von Monakow segment II of WM. Thirdly, brain MRI was performed on average 2.8 days earlier in the TEA-PN group compared to the TN control group. By missing precise information on cerebral growth kinetics in neonates, we ran a sub-analysis in 21 TEA-PN whose postmenstrual age at MRI was matched to 21 TN (Supplementary Table 2). Results obtained in the TEA-PN sub-group were consistent with those obtained when including all TEA-PN infants confirming that earlier MRI acquisition (on average 2.8 days) is not clinically relevant, although it is statistically significant. Finally, we did not investigate the relationship between the maturational brain level summarized by the cumulative score and the long-term neurodevelopmental outcome.

5. Conclusion

Our data suggest that the brain maturity at term age explored by the radiological aspect of the transient fetal compartments was different in TN compared to PN at TEA. The assessment of the transient fetal compartments depicted a more variable maturation pattern than the only assessment of the usually considered structures. The crossroads visibility and the subplate morphology, less mature in PN at TEA than in TN babies, discriminated particularly well both groups. However, some structures of the WM seem to be more mature in PN at TEA than in TN and open the debate, if a premature birth may accelerate the brain maturation through early multisensorial experiences. The performance of our scoring system to detect TEA-PN at higher risk to

adverse outcome should be evaluated in a large cohort of preterm infants with a known neurodevelopmental outcome.

Declaration of Competing Interest

None.

Supplementary materials

Supplementary material associated with this article can be found, in the online version, at doi:10.1016/j.nicl.2019.102014.

References

Allin, M.P., Kontis, D., Walshe, M., Wyatt, J., Barker, G.J., Kanaan, R.A., McGuire, P., Rifkin, L.L., Murray, R.M.R., Nosarti, C.C., 2011. White matter and cognition in adults who were born preterm. PLoS One 6 e24525-e24525.

Armstrong, D.L., Bagnall, C., Harding, J.E., Teele, R.L., 2002. Measurement of the subarachnoid space by ultrasound in preterm infants. Archives of disease in childhood. Fetal Neonat. Edit. 86, F124–F126.

Back, S.A., Miller, S.P., 2014. Brain injury in premature neonates: a primary cerebral dysmaturation disorder? Ann. Neurol. 75, 469–486.

Ball, G., Boardman, J.P., Rueckert, D., Aljabar, P., Arichi, T., Merchant, N., Gousias, I.S., Edwards, A.D., Counsell, S.J., 2012. The effect of preterm birth on thalamic and cortical development. Cereb. Cortex 22, 1016–1024.

Ball, G., Pazderova, L., Chew, A., Tusor, N., Merchant, N., Arichi, T., Allsop, J.M., Cowan, F.M., Edwards, A.D., Counsell, S.J., 2015. Thalamocortical connectivity predicts cognition in children born preterm. Cereb. Cortex 25, 4310–4318.

Barkovich, A.J., Kjos, B.O., Jackson, D.E., Norman, D., 1988. Normal maturation of the neonatal and infant brain: MR imaging at 1.5 T. Radiology 166, 173–180.

Chau, V.V., Synnes, A.A., Grunau, R.E.R., Poskitt, K.J.K., Brant, R.R., Miller, S.P.S., 2013. Abnormal brain maturation in preterm neonates associated with adverse developmental outcomes. Neurology 81, 2082–2089.

Chi, J.G., Dooling, E.C., Gilles, F.H., 1977. Gyral development of the human brain. Ann. Neurol. 1, 86–93.

Childs, A.M., Ramenghi, L.A., Cornette, L., Tanner, S.F., Arthur, R.J., Martinez, D., Levene, M.I., 2001. Cerebral maturation in premature infants: quantitative assessment using MR imaging. AJNR Am. J. Neuroradiol. 22, 1577–1582.

Dubois, J., Benders, M., Borradori Tolsa, C., Cachia, A., Lazeyras, F., Ha-Vinh Leuchter, R.R., Sizonenko, S.V.R., Warfield, S.K.R., Mangin, J.F.R, Hüppi, P.S.R., 2008a. Primary cortical folding in the human newborn: an early marker of later functional development. Brain 131, 2028–2041.

Dubois, J., Benders, M., Cachia, A., Lazeyras, F., Ha-Vinh Leuchter, R.R., Sizonenko, S.V.R., Borradori Tolsa, C.R, Mangin, J.F.R., Hüppi, P.S.R., 2008b. Mapping the early cortical folding process in the preterm newborn brain. Cereb. Cortex 18, 1444–1454.

Dubois, J., Dehaene-Lambertz, G., Perrin, M., Mangin, J.F., Cointepas, Y., Duchesnay, E., Le Bihan, D., Hertz-Pannier, L., 2008b. Asynchrony of the early maturation of white matter bundles in healthy infants: quantitative landmarks revealed noninvasively by diffusion tensor imaging. Hum. Brain Mapp. 29, 14–27.

Ferrie, J.C., Barantin, L., Saliba, E., Akoka, S., Tranquart, F., Sirinelli, D., Pourcelot, L., 1999. MR assessment of the brain maturation during the perinatal period: quantitative T2 MR study in premature newborns. Magn. Resonan. Imag. 17, 1275–1288.

Fischi Gomez, E., Vasung, L., Meskaldji, D.-E., Lazeyras, F., Borradori Tolsa, C., Hagmann, P., Barisnikov, K., Thiran, J-P., Hüppi, P.S., 2015. Structural brain connectivity in school-age preterm infants provides evidence for impaired networks relevant for higher order cognitive skills and social cognition. Cereb. Cortex 25, 2793–2805.

George, J.M., Boyd, R.N., Colditz, P.B., Rose, S.E., Pannek, K., Fripp, J., Lingwood, B.E., Lai, M., Kong, A.H., Ware, R.S., Coulthard, A., Finn, C.M., Bandaranayake, S.E., 2015. PPREMO: a prospective cohort study of preterm infant brain structure and function to predict neurodevelopmental outcome. BMC Pediatr. 15, 123.

Groppo, M., Ricci, D., Bassi, L., Merchant, N., Doria, V., Arichi, T., Allsop, J.M., Ramenghi, L., Fox, M.J., Cowan, F.M., Counsell, S.J., Edwards, A.D.S., 2014. Development of the optic radiations and visual function after premature birth. Cortex (Testo stampato) 56, 30–37.

Gui, L., Lisowski, R., Faundez, T., Hüppi, P.S., Lazeyras, F., Kocher, M., 2012. Morphology-driven automatic segmentation of MR images of the neonatal brain.

Med. Image Anal. 16, 1565–1579.

Haynes, R.L., Sleeper, L.A., Volpe, J., Kinney, H.C., 2013. Neuropathologic studies of the encephalopathy of prematurity in the late preterm infant. Clin. Perinatol. 40, 707–722.

Horsch, S., Muentjes, C., Franz, A., Roll, C., 2005a. Ultrasound diagnosis of brain atrophy is related to neurodevelopmental outcome in preterm infants. Acta Paediatr. 94, 1815–1821.

Inder, T.E., Wells, S.J., Mogridge, N.B., Spencer, C., Volpe, J., 2003. Defining the nature of the cerebral abnormalities in the premature infant: a qualitative magnetic resonance imaging study. J. Pediatr. 143, 171–179.

Ivica, I., Ivica, M., Sedmak, G., 2011. Developmental history of the subplate zone, subplate neurons and interstitial white matter neurons: relevance for schizophrenia. Int. J. Dev. Neurosci. 29, 193–205.

Ivica, I., Ivica, N., Milan, M., Sedmak, G., Benjak, V., Mirna, M., Vasung, L., Marko, M., Hüppi, P.S., 2014. Perinatal and early postnatal reorganization of the subplate and related cellular compartments in the human cerebral wall as revealed by histological and MRI approaches. Brain Struct. Funct. 219, 231–253.

Ivica, I., Judas, M., 2007. Transient patterns of cortical lamination during prenatal life: do they have implications for treatment? Neurosci. Biobehav. Rev. 31, 1157–1168.

Ivica, I., Judas, M., 2010. The development of the subplate and thalamocortical connections in the human foetal brain. Acta Paediatr. 99, 1119–1127.

Judas, M., Rados, M., Jovanov Milosevic, N., Hrabac, P., Stern Padovan, R., Kostovic, I., 2005. Structural, immunocytochemical, and mr imaging properties of periventricular crossroads of growing cortical pathways in preterm infants. AJNR Am. J. Neuroradiol. 26, 2671–2684.

Karolis, V.R., Froudist Walsh, S., Kroll, J., Brittain, P.J., Tseng, C.J-E., Nam, K.-W., Reinders, A.T.S., Murray, R.M., Williams, S.C.R., Thompson, P.M., Nosarti, C., 2017. Volumetric grey matter alterations in adolescents and adults born very preterm suggest accelerated brain maturation. NeuroImage (Orlando, Fla. Print) 163, 379–389.

Khan, S., Vasung, L., Marami, B., Rollins, C.K., Afacan, O., Ortinau, C.M., Yang, E., Warfield, S.K., Gholipour, A., 2019. Fetal brain growth portrayed by a spatiotemporal diffusion tensor MRI atlas computed from in utero images. Neuroimage 185, 593–608.

Kidokoro, H., Anderson, P.J., Doyle, L.W., Woodward, L.J., Neil, J., Inder, T.E., 2014. Brain injury and altered brain growth in preterm infants: predictors and prognosis. Pediatrics 134, 444–453.

Kinney, H.C., 2006. The near-term (late preterm) human brain and risk for periventricular leukomalacia: a review. Semin. Perinatol. 30, 81–88.

Kinney, H.C., Haynes, R.L., Xu, G., Andiman, S.E., Folkerth, R.D., Sleeper, L.A., Volpe, J., 2012. Neuron deficit in the white matter and subplate in periventricular leukomalacia. Ann. Neurol. 71, 397–406.

Kostovic, I., Judas, M., Sedmak, G., 2011. Developmental history of the subplate zone, subplate neurons and interstitial white matter neurons: relevance for schizophrenia. Int. J. Dev. Neurosci. 29, 193–205.

Kostovic, I., Kostovic-Srzentic, M., Benjak, V., Jovanov-Milosevic, N., Rados, M., 2014. Developmental dynamics of radial vulnerability in the cerebral compartments in preterm infants and neonates. Front. Neurol. 5, 139.

Landis, J.R., Koch, G., 1977. The measurement of observer agreement for categorical data. Biometrics 33, 159–174.

Nguyen The Tich, S., Anderson, P.J., Shimony, J.S., Hunt, R.W., Doyle, L.W., Inder, T.E., 2009. A novel quantitative simple brain metric using MR imaging for preterm infants. AJNR Am. J. Neuroradiol. 30, 125–131.

Oreskovic, D., Klarica, M., 2011. Development of hydrocephalus and classical hypothesis of cerebrospinal fluid hydrodynamics: facts and illusions. Prog. Neurobiol. 94, 238–258.

Paredes, M.F., James, D., Gil Perotin, S., Kim, H., Cotter, J.A., Ng, C., Sandoval, K., Rowitch, D.H., Xu, D., McQuillen, P.S., Garcia Verdugo, J-M., Huang, E.J., Alvarez Buylla, A., 2016. Extensive migration of young neurons into the infant human frontal lobe. Science 354.

Perlman, J.M., 2001. Neurobehavioral deficits in premature graduates of intensive care—potential medical and neonatal environmental risk factors. Pediatrics 108, 1339–1348.

Pogledic, I., Kostovic, I., Fallet Bianco, C., Adle Biassette, H., Gressens, P., Verney, C., 2014. Involvement of the subplate zone in preterm infants with periventricular white matter injury. Brain Pathol. 24, 128–141.

Rados, M., Judas, M., Kostovic, I., 2006. In vitro MRI of brain development. Eur. J. Radiol. 57, 187–198.

Ramenghi, L.A., Martinelli, A., De Carli, A., Brusati, V., Mandia, L., Fumagalli, M., Triulzi, F., Mosca, F., Cetin, I., 2011. Cerebral maturation in IUGR and appropriate for gestational age preterm babies. Reproduct. Sci. 18, 469–475.

Schmidt, B., Roberts, R.S., Davis, P.G., Doyle, L.W., Asztalos, E.V., Opie, G., Bairam, A., Solimano, A., Arnon, S., Sauve, R.S., 2015. Prediction of late death or disability at age 5 years using a count of 3 neonatal morbidities in very low birth weight infants. J. Pediatr. 167, 982–986.

Shimony, J.S., Smyser, C.D., Wideman, G., Alexopoulos, D., Hill, J., Harwell, J., Dierker, D., Van Essen, D.C., Inder, T.E., Neil, J., 2016. Comparison of cortical folding measures for evaluation of developing human brain. NeuroImage (Orlando, Fla. Print) 125, 780–790.

Takahashi, E., Folkerth, R.D., Galaburda, A.M., Grant, P.E., 2012. Emerging cerebral connectivity in the human fetal brain: an MR tractography study. Cereb. Cortex 22, 455–464.

van der Knaap, M.S., van Wezel-Meijler, G., Barth, P.G., Barkhof, F., Adler, H.J., Valk, J.G., 1996. Normal gyration and sulcation in preterm and term neonates: appearance on MR images. Radiology 200, 389–396.

Vasung, L., Jovanov-Milosevic, N., Pletikos, M., Mori, S., Judas, M., Kostovic, I., 2011. Prominent periventricular fiber system related to ganglionic eminence and striatum in the human fetal cerebrum. Brain Struct. Funct. 215, 237–253.

Vasung, L., Huang, H., Hao, N., Pletikos, M., Mori, S., Kostovic, I., 2010. Development of axonal pathways in the human fetal fronto-limbic brain: histochemical characterization and diffusion tensor imaging. J. Anatomy 217, 400–417.

Vasung, L., Lepage, C., Milan, M., Pletikos, M., Goldman, J.S., Richiardi, J., Marina, M., Fischi Gömez, E., Karama, S., Hüppi, P.S., Evans, A.C., Kostovic, I., 2016. Quantitative and qualitative analysis of transient fetal compartments during prenatal human brain development. Front. Neuroanat. 10, 11.

Vasung, L., Raguz, M., Kostovic, I., Takahashi, E., 2017. Spatiotemporal relationship of brain pathways during human fetal development using high-angular resolution diffusion MR imaging and histology. Front. Neurosci. 11, 348.

Volpe, J., 2009. The encephalopathy of prematurity–brain injury and impaired brain development inextricably intertwined. Semin. Pediatr. Neurol. 16, 167–178.

Volpe, J., Kinney, H.C., Jensen, F.E., Rosenberg, P.A., 2011. The developing oligodendrocyte: key cellular target in brain injury in the premature infant. Int. J. Dev. Neurosci. 29, 423–440.

von Monakow, ., 1905. Gehirnpathologie.

Vossough, A., Limperopoulos, C., Putt, M.E., du Plessis, A.J., Schwab, P.J., Wu, J., Gee, J.C., Licht, D.J., 2013. Development and validation of a semiquantitative brain maturation score on fetal MR images: initial results. Radiology 268, 200–207.

Walsh, J.M., Doyle, L.W., Anderson, P.J., Lee, K.J., Cheong, J.L., 2014. Moderate and late preterm birth: effect on brain size and maturation at term-equivalent age. Radiology 273, 232–240.

Woodward, L.J., Anderson, P.J., Austin, N.C., Howard, K., Inder, T.E., 2006. Neonatal MRI to predict neurodevelopmental outcomes in preterm infants. New Engl. J. Med. 355, 685–694.

Yakovlev, PL., Lecours, AR., 1967. The myelinogenetic cycles of regional maturation of the brain. Retional Development of the Brain Early in Life. Blackwell Scientific Publications, pp. 3–70.